NeuroImage: Clinical 20 (2018) 808–822

Contents lists available at ScienceDirect

NeuroImage: Clinical

journal homepage: www.elsevier.com/locate/ynicl

White matter microstructure is associated with language in children born very preterm

Ines M. Mürner-Lavanchy[a,b,i], Claire E. Kelly[b], Natalie Reidy[b], Lex W. Doyle[b,c,e,f], Katherine J. Lee[b,e], Terrie Inder[g], Deanne K. Thompson[b,d,e], Angela T. Morgan[b,e,h], Peter J. Anderson[a,b,*]

[a] Monash Institute of Cognitive and Clinical Neurosciences, Monash University, Australia
[b] Murdoch Children's Research Institute, Melbourne, Australia
[c] Department of Obstetrics and Gynaecology, University of Melbourne, Melbourne, Victoria, Australia
[d] Florey Institute of Neuroscience and Mental Health, Melbourne, Australia
[e] Department of Paediatrics, University of Melbourne, Melbourne, Australia
[f] Research Office, The Royal Women's Hospital, Melbourne, Australia
[g] Harvard Medical School, Boston, USA
[h] Department of Audiology and Speech Pathology, University of Melbourne, Melbourne, Australia
[i] University Hospital of Child and Adolescent Psychiatry and Psychotherapy, University of Bern, Bern, Switzerland.

ARTICLE INFO

Keywords:
Preterm birth
Language
Magnetic resonance imaging
Diffusion-weighted imaging
NODDI

ABSTRACT

Very preterm birth is associated with altered white matter microstructure and language difficulties, which may compromise communication, social function and academic achievement, but the relationship between these two factors is unclear. The aim of this study was to explore associations between white matter microstructure and language domains of semantics, grammar and phonological awareness at 7-years of age on a whole-brain level and within the arcuate fasciculus, an important language pathway, in very preterm and term-born children.

Language was assessed in 145 very preterm-born (< 30 weeks' gestation and/or < 1250 g birth weight) and 33 term-born children aged 7 years. Fractional anisotropy (FA), axial diffusivity (AD), radial diffusivity (RD), mean diffusivity (MD), axon orientation dispersion and axon density were estimated from diffusion magnetic resonance images also obtained at 7 years. The correlation between diffusion values and language was assessed using Tract-Based Spatial Statistics (TBSS). The arcuate fasciculus was delineated using constrained spherical deconvolution tractography and diffusion parameters from this tract were related to language measures using linear regression.

While there was evidence for widespread associations between white matter microstructure and language, there was little evidence of differences in these associations between very preterm and term-born groups. TBSS analyses revealed that higher FA and lower AD, RD, and MD in major fibre tracts, including those subserving language, were associated with better semantic, grammar and phonological awareness performance. Higher axon density in widespread fibre tracts was also associated with better semantic performance. The tractography analyses of the arcuate fasciculus showed some evidence for associations between white matter microstructure and language outcomes.

White matter microstructural organisation in widespread fibre tracts, including language-relevant pathways, was associated with language performance in whole-brain and tract-based analyses. The associations were similar for very preterm and term-born groups, despite very preterm children performing more poorly across language domains.

Abbreviations: VPT, Very preterm; FA, Fractional anisotropy; AD, axial diffusivity; RD, radial diffusivity; MD, mean diffusivity; TBSS, Tract-Based Spatial Statistics; DTI, Diffusion Tensor Imaging; NODDI, Neurite Orientation Dispersion and Density Imaging; GA, gestational age

* Corresponding author at: Monash Institute of Cognitive and Clinical Neurosciences, School of Psychological Sciences, Monash University, 18 Innovation Walk, Clayton, VIC 3800, Australia.

E-mail addresses: ines@lavanchy.de (I.M. Mürner-Lavanchy), peter.j.anderson@monash.edu (P.J. Anderson).

https://doi.org/10.1016/j.nicl.2018.09.020
Received 8 April 2018; Received in revised form 23 August 2018; Accepted 21 September 2018
Available online 22 September 2018

1. Introduction

Very preterm children (VPT; < 32 weeks gestational age [GA]) are at increased risk for language difficulties compared with their term-born peers. On average, these children score between one- and two-thirds of a standard deviation below same-aged peers in expressive and receptive language domains, including vocabulary, morphology, semantics, grammar and phonological processing (Barre et al., 2011; Foster-Cohen et al., 2010; Reidy et al., 2013; van Noort-van der Spek et al., 2012; Wolke et al., 2008). Language difficulties are likely to persist beyond preschool age (Guarini et al., 2009) and may compromise communication, social function, mental health, academic achievement, and career prospects (Carroll et al., 2005).

One important factor potentially contributing to language difficulties in VPT children is the complex amalgam of neural disturbances on the prematurely born infant's brain (Volpe, 2009a). Approximately 50% of VPT infants show diffuse white matter injuries at birth (Cheong et al., 2009; Inder et al., 2003; Miller et al., 2005) which implicate impairments in myelination and axonal development (Volpe, 2009b). These impairments may result in atypical white matter development, with white matter abnormalities persisting into childhood (Lubsen et al., 2011; Ment et al., 2009). Altered microstructural organisation has been demonstrated in many fibre tracts in VPT populations throughout infancy, childhood, adolescence and young adulthood (Pandit et al., 2013; Thompson et al., 2014).

Altered white-matter architecture following preterm birth has been related to a range of outcomes including motor skills, cognition, behaviour, speech and language (Constable et al., 2013, 2008; Murray et al., 2016; Skranes et al., 2007; Thompson et al., 2014), with perinatal white matter abnormalities also reported to be associated with impaired language abilities in children born VPT (Reidy et al., 2013). Further, white matter microstructure, namely higher fractional anisotropy (FA), in widespread brain regions has been associated with better performance in verbal IQ, linguistic processing speed, syntax performance, speech and oromotor outcome in adolescent preterm (< 36 GA) and VPT individuals (Feldman et al., 2012; Northam et al., 2012a). Higher FA in several major white matter tracts has also been related to better reading performance in VPT adolescents, but to worse performance in term-born controls (n = 19) (Travis et al., 2016). In a recent study with 3–5 year-old typically developing children, higher FA and lower MD in several tracts was correlated with phonological processing skills (Walton et al., 2018). Given the important role of language for everyday functioning and vocational achievement, understanding the contributing factors to language outcomes in preterm children, including underlying white-matter microstructure, may be important for future clinical prognostication.

The microstructural organisation of white matter can be measured non-invasively using diffusion tensor imaging (DTI), which provides voxel-wise quantitative parameters based on water diffusion properties of the brain. Conventional diffusion tensor parameters include FA, a metric of directional restriction of diffusion, axial diffusivity (AD), reflecting diffusion along the prominent diffusion orientation, radial diffusivity (RD), measuring diffusion perpendicular to the prominent diffusion orientation and mean diffusivity (MD), which indicates the degree of overall diffusion within a voxel (Jones et al., 2013). Diffusion restriction in the white matter depends on many factors such as myelination, axon diameter, membrane permeability, axon density and axon orientation distribution (Jones et al., 2013). Recently developed techniques such as Neurite Orientation Dispersion and Density Imaging (NODDI) allow a more direct examination of the underlying cellular microstructural properties of the diffusion signal compared with DTI (Zhang et al., 2012). NODDI is a technique which enables the extraction of two key values possibly underlying changes in diffusion tensor parameters in the white matter: axon orientation dispersion and axon density (Zhang et al., 2012). Using NODDI, our previous work identified that lower white matter FA after prematurity can be associated with increases in axon dispersion and decreases in axon density (Kelly et al., 2016).

Advances in differentiating fibre tracts associated with language using tractography allowed determination of three major language pathways: 1) a ventral fibre tract connecting the superior temporal cortex (Wernicke's area) to the anterior portion of Broca's area (pars triangularis, Brodmann area [BA] 45/47) via the medial temporal gyrus, which has been suggested to be mainly involved in semantic processing (Saur et al., 2008; Turken and Dronkers, 2011); 2) a dorsal fibre tract connecting the superior temporal cortex to premotor cortical areas, which is mainly involved in language production (Catani et al., 2005; Friederici, 2011; Perani et al., 2011); and 3) a second dorsal fibre tract, connecting the superior temporal gyrus to the posterior portion of Broca's area (BA 44), partly running parallel to the pathway described in 2). This tract, which is suggested to be mainly responsible for syntactical processing and complex sentence structure, comprises the arcuate fasciculus (Friederici et al., 2017; Skeide et al., 2016, 2014). While pathways 1 and 2 develop early in life, pathway 3 is thought to develop into late childhood (Brauer et al., 2011; Friederici et al., 2017; Skeide et al., 2016) and is therefore of particular interest to the study of brain-behaviour relationships in VPT samples, suggested to be delayed in language processing (Barre et al., 2011; Mürner-Lavanchy et al., 2014a; van Noort-van der Spek et al., 2012). Importantly, recent evidence reveals the predictive role of arcuate fasciculus microstructure for individual differences in linguistic abilities in two-year-old VPT children (Salvan et al., 2017). Further, FA of the left arcuate fasciculus has been associated with better phonological awareness in six-year-old VPT and term-born children (Dodson et al., 2018) while in 7–11-year-old typically developing children, higher FA and lower RD in the left arcuate fasciculus correlated with worse phonological awareness (Yeatman et al., 2011).

Previous studies in VPT children have investigated white matter microstructural correlates of language using developmental tests (Salvan et al., 2017) or focused on reading and precursors of reading skills, such as phonological processing (Travis et al., 2016; Walton et al., 2018). We chose to extend the current literature by examining the microstructural correlates of phonological processing and two additional fundamental language domains of semantics and grammar. Early school-age is an ideal age range to investigate associations between white matter microstructure and language, as core language domains can be reliably assessed and development of complex language function is ongoing.

The aim of this study was to explore the association between white matter microstructural parameters and language outcomes in VPT and term-born 7 year-olds and whether these relationships differed in the two birth groups. Specifically, the first aim was to examine the association between whole brain white matter tracts and language performance in sub-domains of semantics, grammar and phonological awareness using Tract-Based Spatial Statistics (TBSS). The second aim was to investigate the association between arcuate fasciculus white matter microstructure and language in VPT and term-born children using tractography.

2. Methods

2.1. Participants

Participants were VPT infants (GA < 30 weeks and/or birth weight < 1250 g) admitted to the Royal Women's Hospital, Melbourne, from July 2001 to December 2003 and recruited into a prospective longitudinal cohort study called the Victorian Infant Brain Study (VIBeS). Infants with genetic or congenital abnormalities likely to interfere with development were excluded (e.g. craniosynostosis, septo-optic dysplasia). During the recruitment period, 348 eligible VPT infants were admitted to the neonatal nursery and 224 (65%) were recruited. The term-born control group comprised of 46 children born at

term (37 to 42 weeks' GA) to women who had uncomplicated pregnancies, and were of normal birth weight (≥2500 g). Term-born infants were recruited at birth from maternity wards at the Royal Women's Hospital, Melbourne or from within the community.

Children in the VIBeS cohort have been followed-up at 2, 5 and 7 years. At the 7-year follow-up, 198 (88%) of VPT children and 43 (94%) of the term-born children were assessed for language outcomes, of which 159 VPT and 36 term-born children also underwent MRI. Attrition was primarily due to families moving interstate/overseas (n = 3), families being uncontactable (n = 3), parents declining follow-up (n = 11) or withdrawing from the study (n = 10). Of the participants who were scanned, we excluded those who did not have the total number of diffusion gradient directions acquired and/or whose final reconstructed images (FA, etc.) had severe motion or other imaging artefact, as previously reported (Kelly et al., 2016). A total of 17 participants were excluded from the TBSS analysis and a further two participants were excluded from the tractography analysis. This left 145 VPT and 33 term-born children who had diffusion scans of sufficient quality to be included in the TBSS analysis, and 143 VPT and 33 term-born children who had diffusion scans of sufficient quality to be included in the tractography analysis.

2.2. Procedure and neurodevelopmental assessment

The original VIBeS study and the follow-up studies were approved by the Human Research and Ethics Committees of the Royal Women's Hospital and the Royal Children's Hospital, Melbourne. Written consent was obtained from the parents for all phases of the study. During the neonatal period, medical data were collected from the infants' health records.

At the 7-year follow-up, families attended appointments over 2 days, with the children having a medical appointment, a cognitive assessment conducted by a trained clinician, a mock MRI scan to familiarise the child with the scanning environment, and a brain MRI. The primary caregiver completed questionnaires to obtain family data. All assessments were conducted by assessors who were blinded to birth group.

2.3. Language assessment

Language was assessed using age-standardised measures based on the child's age corrected for prematurity, each with acceptable test-retest reliability and content validity (Korkman et al., 2007; Semel et al., 2006). Semantic processing was assessed with the Language Content Index (LCI) from the Clinical Evaluation of Language Fundamentals – Fourth Edition – Australian Standardised Edition (CELF-4) (Wiig and Secord, 1989). Grammar was evaluated with the Language Structure Index (LSI) from the CELF-4. Both LCI and LSI have a mean of 100 and standard deviation (SD) of 15. Phonological awareness was assessed with the Phonological Processing subtest of the "A Developmental NEuroPSYchological Assessment" - NEPSY-II (Korkman et al., 2007), which has a mean scaled score of 10 and SD of 3. Children who were too impaired to participate in or understand a particular test were assigned a raw score of 0, corresponding to a scaled score of 40 for the subdomains of semantics and grammar and a scaled score of 1 for the test of phonological awareness.

2.4. MRI data acquisition

Whole brain images were acquired on a 3 Tesla Siemens Magnetom Trio (Tim system) scanner, at the Royal Children's Hospital, Melbourne. Two echo planar diffusion sequences with b values of 1200 and 3000 were used for the current study. The first diffusion protocol was acquired with T_R = 12,000 ms, T_E = 96 ms, field of view = 250 × 250 mm, matrix = 144 × 144, 1.7 mm^3 isotropic voxels, one image with b-value = 0 s/mm^2, and 25 gradient directions with b-values up to 1200 s/mm^2. The second diffusion protocol was acquired with T_R = 7600 ms, T_E = 110 ms, field of view = 240 × 240 mm, matrix = 104 × 104, 2.3 mm^3 isotropic voxels, six images with b-value = 0 s/mm^2, 45 gradient directions with b-value = 3000 s/mm^2.

2.5. Preprocessing and Model Fitting

The diffusion tensor data were generated from the b1200 sequence. All pre-processing for diffusion tensor imaging was performed using the Functional MRI of the Brain Software Library (FSL) version 5.0.8. Firstly, motion and eddy current induced distortion correction was performed (using the "eddy_correct" tool), along with subsequent re-orienting of the b-vectors (Leemans and Jones, 2009). Next, the weighted linear least squares tensor fitting method was employed (Veraart et al., 2013). This generated FA, AD, RD and MD maps in b = 1200 s/mm^2 space (i.e. with a voxel size of 1.7mm^3).

The NODDI data were generated from the b1200 and b3000 sequences. All pre-processing for NODDI was performed using FSL. Because the b1200 and b3000 sequences were separate acquisitions and had different voxel sizes, we registered the b3000 images to the b1200 images (Jenkinson et al., 2002) and then merged the b3000 images with the b1200 images. The combined images were motion and eddy current distortion corrected (using the "eddy_correct" tool). After motion correction, to account for the different TEs between the b1200 and b3000 images, each sequence was normalised by the b = 0 s/mm^2 image for that sequence, as previously described (Kelly et al., 2016). The specific steps in the TE normalisation were: 1. the combined, motion corrected b1200 and b3000 sequences were split up; 2. each separate sequence (including all its volumes, i.e. b = 0 s/mm^2 and diffusion-weighted volumes) was divided by the b = 0 s/mm^2 image for that sequence on a voxel-wise basis using a 'fslmaths' command (in the case of the b3000 sequence, six b = 0 s/mm^2 images were acquired, so these were firstly averaged, and then the b3000 sequence was divided by the average b = 0 s/mm^2 image); 3. the resulting normalised sequences were merged back together. Following TE normalisation, NODDI model fitting was performed using the NODDI Matlab toolbox version 0.9 (Zhang et al., 2012). NODDI model fitting generated neurite orientation dispersion and density maps in b = 1200 s/mm^2 space (i.e. with a voxel size of 1.7mm^3).

No individual diffusion volumes were removed during pre-processing; rather participants were excluded if their final reconstructed images exhibited severe motion artefact based on visual inspection.

2.6. Tract-based spatial statistics

TBSS was used within FSL (Smith et al., 2006) to analyse FA, AD, MD, RD, axon dispersion and axon density. Using FSL's nonlinear registration tool (FNIRT) (Andersson et al., 2007a, 2007b), each participant's FA image was aligned to that of every other participant. The most representative FA image (i.e. the image which required the least warping to all other participants) was identified as the study-specific target (template) FA image. Using affine registration, the target was then aligned to MNI152 1x1x1 mm standard space, and every participant's FA image was transformed from their native space (i.e. b1200 space) into the space of the 1x1x1 mm MNI152 template. A mean FA image and mean FA skeleton were then generated with a threshold of 0.2. Each aligned FA image was projected onto the mean FA skeleton. Original nonlinear registrations were also applied to the MD, RD, AD, axon dispersion and density images, and these images were then projected onto the mean FA skeleton.

2.7. Probabilistic tractography

The constrained spherical deconvolution (CSD) technique (Tournier et al., 2007) was utilised to conduct tractography on b = 3000 diffusion images, using the MRtrix Version 0.2.10 software package (Tournier,

2010). Brain masks were first created to remove non-brain matter. To perform CSD, the response function was estimated from voxels with FA over 0.6, assumed to have single-fibre orientations, and a maximum harmonic order of 6 was used (Tournier et al., 2004). To identify the arcuate fasciculus, two regions of interest (ROIs) were identified for each tract by N. R. (Online Supplementary Fig. S1). Locations of the ROIs were identified on a colour-coded principal eigenvector map, using similar imaging slice locations to previous studies in adults and children (Bernal and Altman, 2010; Hong et al., 2009; Lebel and Beaulieu, 2009; Matsumoto et al., 2008). For the anterior ROI, the widest section of the anterior component of the arcuate fasciculus was located on an axial slice, lying lateral to the corona radiata and superior to the insula. This was usually at or near the coronal slice that identified the transverse pontine fibres. The ROI was then drawn on the coronal slice. The posterior ROI was identified and drawn at the superior-to-inferior component of the tract located lateral to the inferior fronto-occipital fasciculus on an axial slice, and confirmed on the sagittal slice. This was done for both the left and right hemispheres.

Probabilistic tractography was conducted using the CSD map, identifying 1000 streamlines per tract. Resulting tracts were then thresholded to remove voxels that were unlikely to be part of the tract; the probability was set to 0.01 (i.e. voxels containing < 10/1000 streamlines were removed). Since the tracts were generated in b3000 space and the diffusion tensor and NODDI maps were in b1200 space, we registered the thresholded, binarised tracts to b1200 space using the Advanced Normalisation Tools (ANTs) toolkit (Avants et al., 2008), multiplied the tracts in b1200 space by the diffusion tensor and NODDI maps, and averaged the values within each participant's entire tract to obtain a single measure of FA, MD, RD, AD, axon dispersion and axon density for the arcuate fasciculus for each participant. Inter-rater reliability was performed by repeating ROI placement and arcuate tractography for $n = 20$ subjects, in a blinded manner. Intraclass correlation coefficients were ≥ 0.97 for diffusion measures within the arcuate fasciculus.

2.8. Statistical analyses

Voxel-wise statistical analyses of the skeletonised FA, AD, MD, RD, axon dispersion and density images were performed using Randomise (version 2.9), FSL's tool for nonparametric permutation- based testing of neuroimaging data (Nichols and Holmes, 2002; Winkler et al., 2014). General linear models with language function as the independent variable, the diffusion parameters as dependent variables and age at scan as a covariate were fitted separately for each language variable (semantics, grammar, phonological awareness) to determine whether language was associated with diffusion values fitted to all children. Further, an additional model was constructed to test whether the association between diffusion variables and language differed between VPT and term-born children by including an interaction between the diffusion measure and birth group.

Three secondary analyses were conducted. 1) The general linear model was repeated controlling for age, sex, language spoken at home (English vs. some English vs. no English) and parental education (tertiary education vs. lower grades of education [≤12 years of formal schooling/trade qualification/qualification without university degree]) to examine the potential influence of these measures on our findings. 2) The general linear model was repeated controlling for age, sex, language spoken at home, parental education and head movement. To examine potential confounding effects of head movement on the TBSS results, we calculated measures of head motion from the output of the motion/eddy-current distortion correction. The absolute displacement (i.e. relative to the first volume) averaged over all the volumes in the b1200 sequence, i.e. the sequence the diffusion tensor parameters were generated from, was used as a covariate in the models for DTI measures (FA, AD, RD and MD). The absolute displacement of the b1200 and b3000 sequences was used as a covariate in the models for NODDI measures, since the NODDI parameters were generated from both sequences. 3) In a third secondary analysis, we excluded children who had intraventricular haemorrhage (IVH) grade III or IV ($n = 5$), cystic periventricular leucomalacia (n = 5), were unable to complete the phonological processing task ($n = 1$) and who had very low IQ (2 SD < term-born group mean, $n = 4$), to examine whether the exclusion of children with major brain pathologies or functionally impaired children influenced our results.

In all statistical tests, 5000 permutations were performed. All results are reported at $p < .05$ after threshold-free cluster enhancement (TFCE) (Smith and Nichols, 2009) and family-wise error rate correction. Analyses were not corrected for multiple comparisons across white matter microstructure parameters. Regions of statistical significance were identified using the John Hopkins University (JHU) white-matter tractography atlas and the JHU International Consortium of Brain Mapping DTI-81 white matter label atlas (Hua et al., 2008).

Statistical analyses of arcuate fasciculus FA, AD, MD, RD, axon dispersion and density were conducted using Stata 14.2 (StataCorp, 2013). The association between arcuate fasciculus parameters and language was assessed using linear regression fitting a separate model for each predictor-outcome combination and using separate models for each MRI parameter for each hemisphere with age at scan as covariate. Models were fitted using generalised estimating equations with results reported with robust standard errors to allow for clustering of multiples within a family (i.e., twins/triplets) (Carlin et al., 2005). Further, birth group-by-microstructural parameter interactions were included to assess whether the relationship between the MRI parameters and language outcome differed between VPT and term-born children. Three secondary analyses were conducted: 1) The regression model was repeated controlling for age, sex, language spoken at home and parental education, to examine the potential influence of these measures on the associations between arcuate diffusion values and language outcomes. 2) To examine potential confounding effects of head motion, we performed secondary analyses controlling the association between arcuate fasciculus parameters and language for age, sex, language spoken at home and parental education, as well as the mean absolute displacement of the b3000 sequence, since the tracts were generated in b3000 space. 3) We repeated the regression model, excluding children with IVH grade III or IV, cystic periventricular leucomalacia, children who had very low IQ and a child who was unable to complete the phonological processing task. Interpretation of our findings in the arcuate fasciculus analysis was based on overall patterns and magnitudes of differences and associations, rather than p-values alone (Wasserstein and Lazar, 2016).

3. Results

3.1. Participant characteristics

Compared with VPT participants, VPT non-participants were more likely to be exposed to postnatal corticosteroids (4.9% participants vs. 17.3% non-participants; Online Supplementary Table S1) and had a longer hospital stay (78 days median for participants vs. 86 days median for non-participants). Other perinatal characteristics (GA at birth, birth weight, proportions of females, IVH grade III/IV, cystic periventricular leukomalacia (PVL), bronchopulmonary dysplasia, antenatal corticosteroid exposure, patent ductus arteriosus and small for GA births) were similar between VPT participants and VPT non-participants. Perinatal characteristics were also similar between term-born participants ($n = 33$) and term-born non-participants ($n = 13$).

Characteristics of the 145 VPT and 33 term-born participants are shown in Table 1. As expected, the VPT group differed from the term-born group with respect to most perinatal characteristics. Measures of semantic performance were obtained in 141 VPT and all 33 term-born children, grammar performance in 140 VPT and 32 term-born children, and phonological awareness in 141 VPT and 33 term-born children at

Table 1
Participant characteristics.

Variable	Very Preterm (n = 145)	Term-born (n = 33)
Gestational age at birth (weeks) – median (range)	28 (10)	39 (4)
Birth weight (g) – median (range)	955 (1011)	3300 (1900)
Females – n (%)	74 (51.7)	17 (51.5)
Singleton – n (%)	72 (50.3)	31 (93.9)
IVH grade III/IV – n (%)	5 (3.5)	0 (0)
Cystic PVL – n (%)	5 (3.5)	0 (0)
BPD – n (%)	43 (30.1)	0 (0)
Postnatal corticosteroids – n (%)	7 (4.9)	0 (0)
Antenatal corticosteroids – n (%)	127 (88.8)	0 (0)
Patent ductus arteriosus – n (%)	67 (46.9)	0 (0)
Small for gestational age – n (%)	12 (8.4)	1 (3.0)
Length of hospital stay (days) – median (IQR)	78 (30)	5 (2)
Age at 7-year scan (years) – mean (SD)	7.5 (0.3)	7.6 (0.2)
Language Content Index – mean (SD)[a]	97.8 (15.2)	110.1 (9.4)
Language Structure Index – mean (SD)[b]	95.6 (15.6)	107.4 (12.2)
Phonological Processing – mean (SD)[c]	9.6 (3.1)	10.8 (2.6)

BPD = bronchopulmonary dysplasia; IQR = inter-quartile range; IVH = intraventricular haemorrhage, PVL = periventricular leukomalacia; SD = standard deviation.
[a] Missing data in 2 children.
[b] missing data in 5 children
[c] missing data in 2 children.

the 7-year assessment; the VPT children performed more poorly in semantics (mean difference [MD] =12.3, $p < .001$), grammar (MD = 11.8, $p < .001$) and phonological awareness (MD = 1.3, $p = .031$).

White matter characteristics of the arcuate fasciculus for VPT and term-born groups are shown in the Online Supplementary Table S2. Additionally, VPT children showed higher values of head motion (absolute and relative mean displacement of the b3000 sequence) than term-born peers (Online Supplementary Table S3). The amount of movement in our sample was similar to previously reported values for term-born and VPT children of similar ages, scanned with similar sequences (Nagy et al. 2003; Yendiki et al. 2014).

3.2. Whole brain white matter microstructure and language performance

Looking at the group as a whole, higher FA, higher axon density, and lower AD, RD and MD in major association, projection and commissural fibre tracts, including language-relevant tracts of the superior and inferior longitudinal fasciculus, inferior fronto-occipital fasciculus and uncinate fasciculus were associated with better semantic performance (Fig. 1 and Table 2). There was little evidence that these relationships differed by birth group (VPT vs. control; i.e. there was little evidence for group interactions).

When controlling for age, sex, language spoken at home and parental education, results remained similar, except for slightly more widespread associations between FA, axon density and AD and semantics (Fig. 2). There was little evidence for group interactions after controlling for these confounding variables.

Adding head motion in the analysis model did not substantially change any of the results (Online Supplementary Fig. S2). Further, there was little evidence that the relationships differed by birth group after controlling for head motion.

After excluding children with major brain pathology and low IQ (n = 14), most associations weakened and only FA in the uncinate fasciculus, superior longitudinal fasciculus, inferior fronto-occipital fasciculus and external capsule showed above threshold associations with semantic performance (Fig. 2). There was little evidence of group interactions after exclusion of children with major brain pathology and low IQ.

Higher FA, and lower AD, RD and MD in many widespread major white matter tracts were associated with better grammar performance (Fig. 3, Table 2). There was little evidence that these relationships differed by birth group.

When adjusting for age, sex, language spoken at home and parental education, results remained similar, except for weaker associations between FA and grammar and additional associations between axon density and grammar (Fig. 2). There was still little evidence of group interactions after adjusting for these variables.

Adding head motion in the model resulted in weaker associations between FA and grammar and stronger associations between axon density and grammar (previously below threshold) (Online Supplementary Fig. S2) and there was still little evidence of group interactions.

After excluding children with major brain pathology and low IQ (n = 14), only RD in the corpus callosum, external capsule, posterior thalamic radiation, inferior fronto-occipital, superior longitudinal and right uncinate fasciculus, showed above threshold associations with grammar performance (Fig. 2). There was little evidence for interactions by birth group after excluding these children.

Higher FA, and lower AD, RD and MD in widespread major white matter tracts were associated with better phonological awareness (Fig. 4, Table 2). There was little evidence that these relationships varied by birth group.

When controlling for age, sex, language spoken at home and parental education, evidence weakened slightly, with weaker associations between AD and phonological awareness (Fig. 2). There was little evidence of group interactions after controlling for these confounding variables.

Adding head motion in the model resulted in weaker and less widespread associations between FA, AD and phonological awareness (Online Supplementary Fig. S2); however, a small association between axon density and phonological awareness appeared. There was little evidence for interactions by birth group after controlling for head motion.

After excluding children who had major brain pathology, low IQ or were unable to complete the task (n = 15), only FA in the corpus callosum, cingulum, inferior fronto-occipital, right superior longitudinal and uncinate fasciculus as well as RD in corona radiata, posterior thalamic radiation, cerebellar peduncle, corticospinal tract, left inferior fronto-occipital, superior longitudinal and right uncinate fasciculus showed above threshold associations with phonological awareness (Fig. 2). There was little evidence for group interactions after excluding these children.

3.3. Arcuate fasciculus white matter microstructure and language performance

There was some evidence that higher arcuate fasciculus FA and axon density and lower RD, MD and axon dispersion were associated with semantic performance in all children (Table 3). There was some evidence that higher arcuate fasciculus FA and lower axon dispersion were associated with grammar performance. Further, there was evidence that higher left arcuate fasciculus FA and lower left arcuate fasciculus axon dispersion correlated with phonological awareness.

Strengths of associations and p-values changed only slightly when controlling for age, sex, language spoken at home, parental education and head motion, or when excluding children with major brain pathology or low IQ and the direction of associations remained the same in these secondary analyses.

There was weak evidence that the relationships varied by birth group (2 out of 36 associations with an uncorrected $p < .05$; Online supplementary Table S4). Evidence of a group interaction was even weaker when controlling for age, sex, language spoken at home, parental education and head motion, or when excluding children who had major brain pathology, low IQ or were unable to complete the language

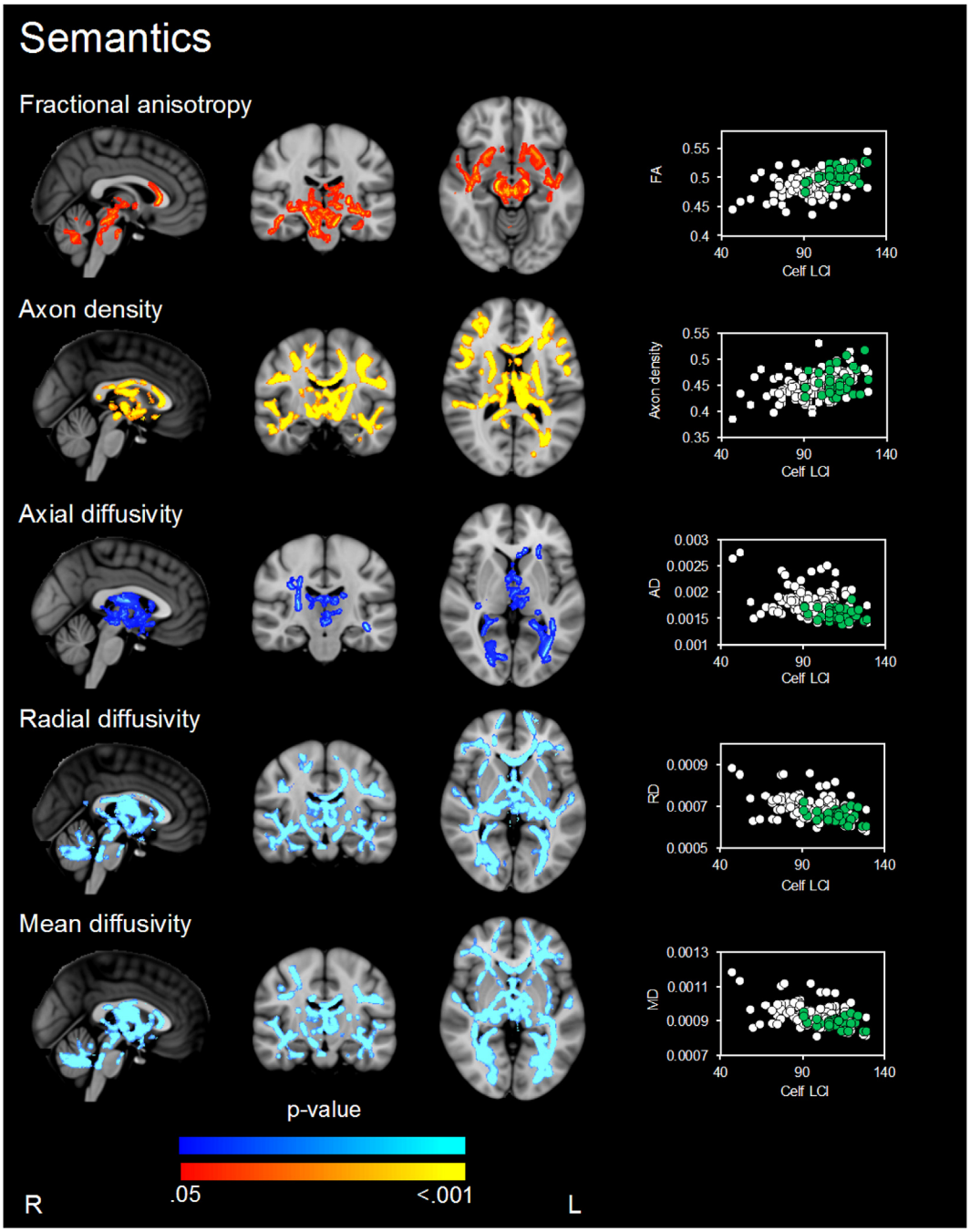

Fig. 1. Regions where there is evidence ($p < .05$, family-wise error corrected) of associations between white matter microstructure parameters and semantic performance when assessed in all children. *P*-values in red-yellow = positive correlations and dark to light blue = negative associations. P-value maps have been overlaid on the standard space (MNI152) T1-weighted image. The scatter plots show the average diffusion value (y-axis) from the significant regions for each participant against semantic performance (x-axis) for each participant (VPT in white and term-born children in green). Only associations, where $p < .05$, after threshold-free cluster enhancement (TFCE) and correction for the family-wise error rate (FWE), are shown. Analyses were not corrected for multiple comparisons across white matter microstructure parameters.

task.

4. Discussion

We found that whole brain white matter microstructure in widespread areas of the brain comprising several major white matter tracts was associated with language performance in the sub-domains of semantics, grammar and phonological awareness. We further found evidence for associations between white matter microstructure of the arcuate fasciculus and language in VPT and term-born children.

Higher FA and axon density, but lower AD, RD and MD in major fibre tracts, including the corpus callosum, internal and external capsule, thalamic radiation, corticospinal tract, fornix, cingulum, superior and inferior longitudinal fasciculus, inferior fronto-occipital fasciculus and uncinate fasciculus were associated with better language performance in our study. Previous studies have found that FA increases and AD, RD and MD decrease over time during typical childhood development. Higher FA has also been related to better language outcomes in several brain regions in term-born (Saygin et al., 2013; Vandermosten et al., 2015; Vandermosten et al., 2012; Walton et al., 2018) and VPT

Table 2
Associations between white matter microstructure and language in very preterm and term-born children.

	Semantic performance					Grammar performance					Phonological awareness				
	FA	AD	RD	MD	Density	FA	AD	RD	MD	Density	FA	AD	RD	MD	Density
Direction of correlation	pos.	neg.	neg.	neg.	pos.	pos.	neg.	neg.	neg.	N/A	pos.	neg.	neg.	neg.	N/A
Total number of voxels (% skeleton)	15,945 (8.2)	9941 (5.1)	52,553 (27)	47,059 (24.2)	43,264 (22.2)	30,191 (15.5)	18,293 (9.4)	49,890 (25.6)	39,272 (20.2)	N/A	47,662 (24.5)	25,953 (13.3)	67,636 (34.7)	72,686 (37.3)	N/A
Cerebellar peduncle superior	✓			✓		✓		✓	✓R		✓	✓	✓	✓	
Cerebellar peduncle middle	✓		✓	✓		✓	✓	✓	✓		✓	✓	✓	✓	
Cerebellar peduncle inferior	✓			✓		✓		✓	✓		✓	✓	✓	✓	
Pontine crossing tract	✓			✓			✓								
Corpus callosum (genu, body, splenium)	✓	✓	✓	✓	✓	✓	✓	✓	✓		✓	✓	✓	✓	
Fornix (column, body, cres/Stria terminalis)	✓	✓	✓	✓	✓	✓	✓	✓	✓		✓	✓	✓	✓	
Corticospinal tract	✓	✓	✓	✓	✓	✓	✓	✓	✓R		✓	✓R	✓	✓	
Medial lemniscus	✓		✓	✓		✓	✓	✓	✓		✓	✓R	✓	✓	
Cerebral peduncle			✓		✓				✓		✓				
Internal capsule (anterior, posterior, retrolenticular)	✓	✓	✓	✓	✓	✓	✓	✓	✓		✓	✓	✓	✓	
Corona radiata (anterior, superior, posterior)	✓	✓	✓	✓	✓	✓	✓	✓	✓		✓	✓	✓	✓	
Thalamic radiation (anterior, posterior)	✓	✓	✓	✓	✓	✓	✓	✓	✓		✓	✓ L	✓	✓	
Sagittal stratum	✓	✓L	✓	✓	✓	✓	✓	✓	✓		✓	✓	✓	✓	
External capsule	✓	✓	✓	✓	✓	✓	✓	✓	✓		✓	✓	✓	✓	
Cingulum (cingulate gyrus, hippocampus)	✓	✓	✓	✓	✓	✓	✓	✓HC	✓		✓	✓	✓	✓	
Forceps (major, minor)	✓	✓	✓	✓	✓	✓	✓	✓	✓		✓	✓	✓	✓	
Longitudinal fasciculus superior	✓	✓	✓	✓	✓	✓	✓	✓	✓		✓	✓	✓	✓	
Longitudinal fasciculus inferior	✓		✓	✓		✓	✓	✓	✓		✓	✓		✓	
Fronto-occipital fasciculus superior		✓	✓	✓	✓	✓		✓R			✓	✓R	✓	✓ R	
Fronto-occipital fasciculus inferior	✓	✓	✓	✓	✓	✓	✓	✓	✓		✓	✓		✓	
Uncinate fasciculus	✓	✓	✓	✓	✓	✓	✓	✓	✓		✓	✓		✓	
Tapetum		✓R	✓	✓		✓		✓	✓		✓	✓R	✓ R	✓ R	

Note. FA, fractional anisotropy AD, Axial diffusivity, RD, radial diffusivity, MD, mean diffusivity. Tick mark implies evidence of an association ($p < .05$, family wise error rate corrected) between the microstructural parameter within that region and language. Associations were identified in both the left (L) and right (R) hemispheres of the brain unless otherwise stated. HC = evidence of an association was found in the hippocampal part of the cingulum only. The axon dispersion parameter was not included in this table because there was no evidence of associations between axon dispersion and language. N/A there was no association between this parameter and language at $p < .05$, family-wise error rate corrected).

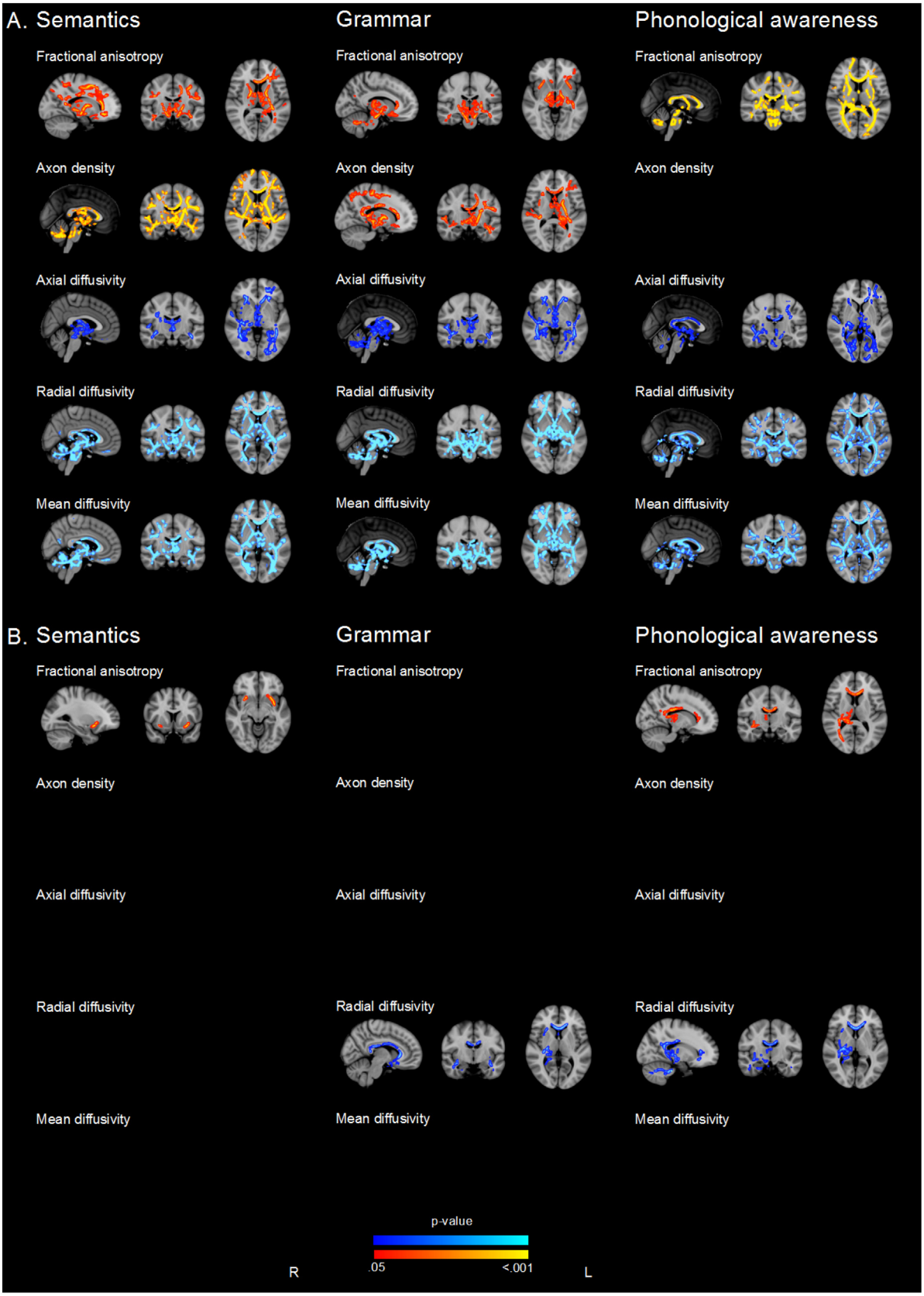

Fig. 2. Regions where there is evidence ($p < .05$, family wise error rate corrected) of A. associations between white matter microstructure parameters and language when assessed in all children, corrected for age, sex, language spoken at home and parental education and B. associations between white matter microstructure parameters and language in children without major brain pathologies, very low IQ and lowest possible language score. *P*-values in red-yellow = positive correlations and dark to light blue = negative associations. P-value maps have been overlaid on the standard space (MNI152) T1-weighted image. Note, no image is shown when no voxels were identified at $p < .05$ family wise error rate-corrected. Analyses were not corrected for multiple comparisons across white matter microstructure parameters.

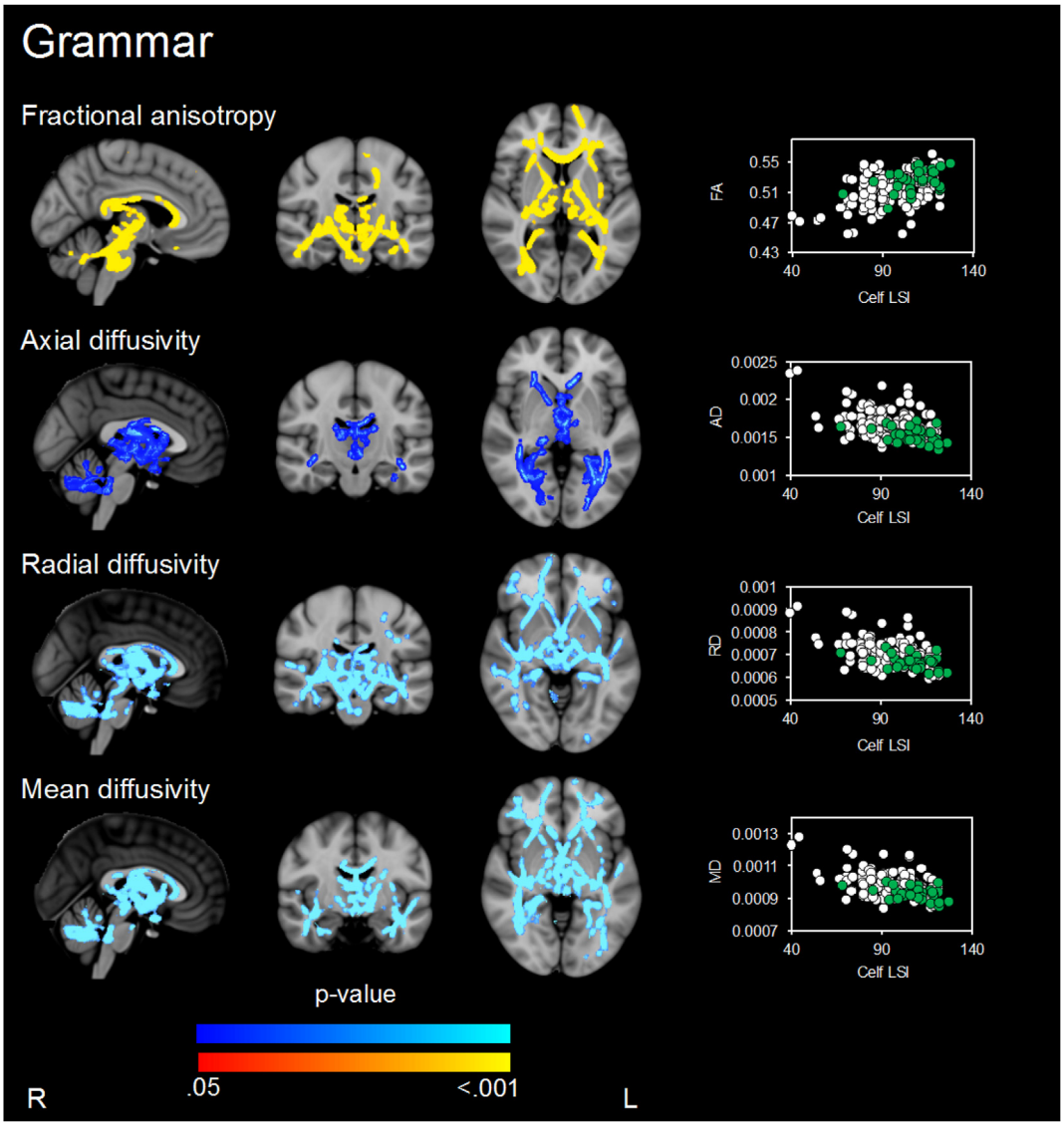

Fig. 3. Regions where there is evidence ($p < .05$, family wise error rate corrected) of associations between white matter microstructure parameters and grammar performance when assessed in all children. *P*-values in red-yellow = positive correlations and dark to light blue = negative associations. P-value maps have been overlaid on the standard space (MNI152) T1-weighted image. The scatter plots show the average diffusion value (y-axis) from the significant regions for each participant against grammar performance (x-axis) for each participant (VPT in white and term-born children in green). Only associations, where $p < .05$, after threshold-free cluster enhancement (TFCE) and correction for the family-wise error rate (FWE), are shown. Analyses were not corrected for multiple comparisons across white matter microstructure parameters.

children (Feldman et al., 2012; Mullen et al., 2011). These previous studies support that higher FA and lower AD, RD and MD are reflective of more mature microstructural organisation of white matter fibre tracts, and support better cognitive outcomes in children. Hence, consistent with previous studies, microstructural characteristics potentially reflecting a more mature organisation of fibres, as measured using DTI, were associated with better language outcome in our sample of VPT and term-born children.

Interpretation of the underlying cellular changes that might explain the associations between the various DTI parameters and language outcomes is challenging. DTI measures are highly sensitive but non-specific, in that they cannot sensitively distinguish between different cellular properties including myelination, axon packing density, axon size or diameter, and axon coherence or geometry (Jones et al., 2013). While DTI measures do not reflect any single aspect of white matter microstructure, it has been suggested that AD may relate more to axonal status and RD may relate more to myelin status (Song et al., 2003), however, all DTI measures are still additionally influenced by axon orientation distributions. To address this limitation in DTI, we complemented our analysis with NODDI, which provides measures that are more specific to axon density and the dispersion of axon orientation distributions compared with DTI (Zhang et al., 2012). Recent studies suggest that axon density increases and axon orientation dispersion remains stable during typical childhood development (Lebel and Deoni, 2018). We previously found that higher axon density was associated with better IQ and motor performance and fewer behavioural problems, while lower axon dispersion was associated with better motor performance and fewer behavioural problems in VPT children (Kelly et al., 2016). In the current paper, we found that higher axon density was related to better semantic performance, but there was less evidence of associations between axon dispersion and language outcomes. While NODDI parameters provide increased specificity to axon density and dispersion compared with DTI, we acknowledge it is difficult to disentangle the separate relationships of the different white matter microstructural parameters with language. Furthermore, while the NODDI parameters provide increased specificity compared with DTI, the

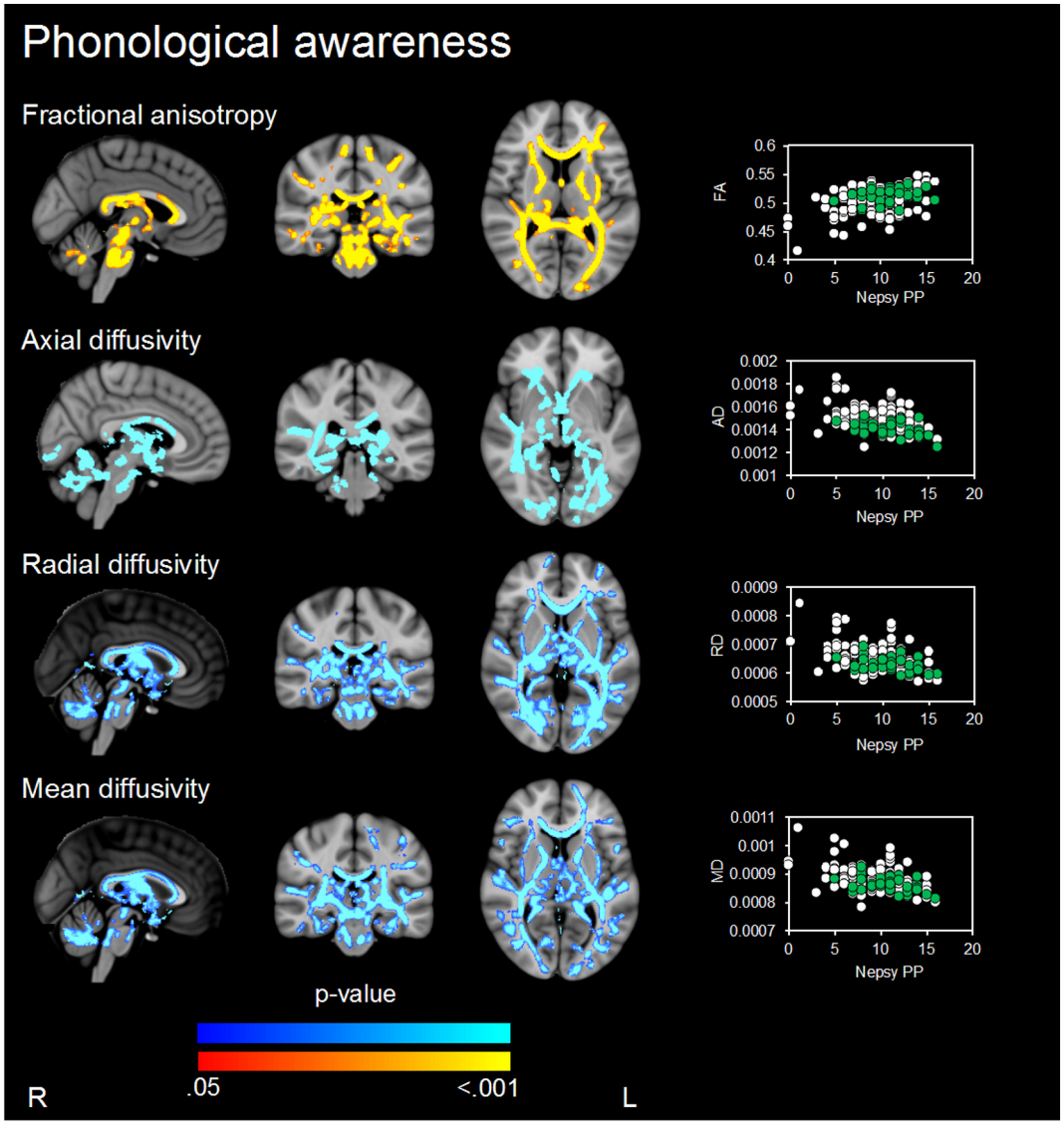

Fig. 4. Regions where there is evidence ($p < .05$, family wise error rate corrected) of associations between white matter microstructure parameters and phonological awareness when assessed in all children. P-values in red-yellow = positive correlations and dark to light blue = negative associations. P-value maps have been overlaid on the standard space (MNI152) T1-weighted image. The scatter plots show the average diffusion value (y-axis) from the significant regions for each participant against phonologic performance (x-axis) for each participant (VPT in white and term-born children in green). Only associations, where $p < .05$, after threshold-free cluster enhancement (TFCE) and correction for the family-wise error rate (FWE), are shown. Analyses were not corrected for multiple comparisons across white matter microstructure parameters.

NODDI axon density measure may still be influenced both by axon density and myelination (Zhang et al., 2012). Studies using MRI acquisitions and analysis techniques that are more sensitive to myelin, such as mcDESPOT (Deoni et al., 2008) or myelin mapping based on the ratio of T_1 and T_2-weighted structural images (Ganzetti et al., 2014; Glasser and Van Essen, 2011) would be highly valuable in future to further disentangle the possible contributions of axonal and myelin status to language outcomes in VPT children. Additionally, in the current study, the NODDI parameters appeared to show fewer associations with language than DTI parameters. This may be due to methodological differences between the techniques, further complicating the direct comparison of DTI and NODDI results. For example, DTI may produce more false positive associations because it is less specific than NODDI and it may suffer more from increased contamination from cerebrospinal fluid compared with NODDI, due to the separate modelling of the cerebrospinal fluid compartment in NODDI (Zhang et al., 2012).

We chose to complement our TBSS analysis with the tractography analysis, because TBSS is highly conservative due to the restriction of the analysis to a tract skeleton and the strict multiple comparison correction, and because tractography is more anatomically specific than TBSS. Probabilistic CSD-based tractography is an advanced technique that allows robust delineation of white matter fibre tracts, even in regions of crossing fibres (Tournier et al., 2012). While previous evidence for associations between arcuate fasciculus white matter microstructure and language performance in VPT children is mixed (Frye et al., 2010; Mullen et al., 2011; Northam et al., 2012b), we found that higher arcuate fasciculus FA and axon dispersion and lower RD, MD and axon density were associated with better semantic performance in the whole group of VPT and term-born children. Higher arcuate fasciculus FA and lower axon dispersion were further related to semantic performance and similar associations appeared in left arcuate fasciculus FA and axon dispersion with phonological awareness. Consequently, similar to the whole-brain analyses using TBSS, our tractography findings suggest that white matter organisation in the arcuate fasciculus is related to better language outcome.

We found evidence that white matter microstructure was associated

Table 3
Associations between the arcuate fasciculus white matter microstructure and language.

Language function	White matter parameter	Hemisphere	Whole group association	*p*-Value	Adjusted whole group association[a]	Adjusted *p*-value[a]	Adjusted whole group association[b]	Adjusted *p*-value[b]	Adjusted whole group association[c]	Adjusted *p*-value[c]
			Estimate (95% CI)		Estimate (95% CI)		Estimate (95% CI)		Estimate (95% CI)	
Semantics	FA	L	144.4 (−25.9, 314.7)	0.10	127.5 (−46.7, 301.7)	0.15	116.9 (−57.1, 290.9)	0.19	144.2 (−26.3, 314.6)	0.10
	FA	R	165.2 (26.8, 303.6)	0.019	157.0 (8.1, 305.9)	0.039	153.1 (3.2, 303.0)	0.045	163.4 (23.8, 303.0)	0.022
	AD	L	1.5 (−65.2, 68.1)	0.97	−14.71 (−89.8, 60.3)	0.70	−13.0 (−89.0, 63.0)	0.74	1.4 (−64.7, 67.6)	0.97
	AD	R	17.5 (−61.5, 96.5)	0.66	2.9 (−80.5, 86.4)	0.95	−5.2 (−90.4, 79.9)	0.90	16.6 (−62.6, 95.8)	0.68
	RD	L	−86.5 (−200.4, 27.5)	0.14	−83.2 (−204.0, 37.5)	0.18	−76.6 (−195.5, 42.4)	0.21	−86.1 (−199.8, 27.6)	0.14
	RD	R	−95.6 (−212.1, 21.0)	0.11	−98.4 (−221.7, 25.0)	0.12	−100.6 (−220.6, 19.4)	0.10	−94.5 (−210.8, 21.9)	0.11
	MD	L	−69.9 (−180.3, 40.6)	0.22	−73.4 (−192.7, 45.8)	0.23	−67.8 (−185.2, 49.6)	0.26	−69.4 (−179.4, 40.5)	0.22
	MD	R	−65.5 (−187.4, 56.4)	0.29	−72.5, (−199.7, 54.7)	0.26	−77.8 (−201.6, 46.0)	0.22	−65.0 (−186.6, 56.6)	0.30
	Axon Density	L	84.2 (−14.4, 182.7)	0.09	77.7 (−16.6, 172.1)	0.11	74.9 (−19.9, 169.7)	0.12	84.5 (−14.1, 183.1)	0.09
	Axon Density	R	71.0 (−8.54, 150.5)	0.08	62.1 (−15.9, 140.0)	0.12	60.2 (−21.4, 141.8)	0.15	70.5 (−9.1, 150.1)	0.08
	Axon Dispersion	L	−163.4 (−323.2, −3.7)	0.045	−121.4 (−278.8, 36.1)	0.13	−91.9 (−257.7, 73.9)	0.28	−165.2 (−326.6, −3.8)	0.045
	Axon Dispersion	R	−257.8 (−417.1, −98.5)	0.002	−230.8 (−395.1, −66.5)	0.006	−195.9 (−377.2, −14.7)	0.034	−258.9 (−418.4, −99.3)	0.001
Grammar	FA	L	196.3 (−26.4, 418.9)	0.08	165.7 (−35.4, 366.9)	0.11	157.8 (−47.7, 363.3)	0.13	195.2 (−29.0, 419.3)	0.09
	FA	R	134.9 (−93.5, 363.4)	0.25	116.4 (−96.7, 329.4)	0.28	112.7 (−105.1, 330.6)	0.31	138.7 (−96.3, 373.7)	0.25
	AD	L	72.5 (−50.6, 195.6)	0.25	63.5 (−37.7, 164.6)	0.22	64.7 (−41.4, 170.7)	0.23	75.8 (−45.0, 196.7)	0.22
	AD	R	62.2 (−63.9, 188.3)	0.33	54.3 (−48.4, 156.9)	0.30	47.6 (59.8, 154.9)	0.39	67.6 (−60.6, 195.8)	0.30
	RD	L	−79.9 (−255.0, 95.0)	0.37	−59.5 (−217.4, 98.3)	0.46	−55.1 (−215.6, 105.3)	0.50	−76.1 (−252.8, 100.5)	0.40
	RD	R	−51.2 (−242.1, 139.7)	0.60	−42.3 (−211.4, 126.8)	0.62	−43.9 (−213.7, 125.9)	0.61	−48.6 (−243.7, 146.4)	0.63
	MD	L	−34.6 (−227.1, 157.9)	0.73	−19.9 (−187.2, 147.4)	0.82	−16.0 (−186.5, 154.5)	0.85	−29.3 (−222.1, 163.6)	0.77
	MD	R	−12.3 (−217.5, 192.9)	0.91	−7.8 (−182.0, 166.4)	0.93	−11.8 (−187.5, 163.8)	0.90	−8.0 (−216.3, 200.2)	0.94
	Axon Density	L	27.9 (−152.1, 207.9)	0.76	14.1 (−153.7, 181.9)	0.87	10.6 (−160.9, 182.1)	0.90	24.8 (−156.2, 205.8)	0.79
	Axon Density	R	28.7 (−114.8, 172.1)	0.70	11.0 (−121.8, 143.9)	0.87	9.4 (−128.5, 147.3)	0.89	26.2 (−119.5, 171.9)	0.73
	Axon Dispersion	L	−294.5 (−529.6, −59.4)	0.014	−251.1 (−460.7, −41.5)	0.019	−230.5 (−449.3, −11.7)	0.039	−305.8 (−546.9, −64.8)	0.013
	Axon Dispersion	R	−329.3 (−580.3, −78.3)	0.010	−229.5 (−528.3, −70.6)	0.010	−274.5 (−513.8, −35.2)	0.025	−352.1 (−615.2, −89.1)	0.009
Phonological awareness	FA	L	28.4 (−11.3, 68.0)	0.16	26.2 (−12.6, 64.9)	0.19	22.1 (−17.2, 61.3)	0.27	28.6 (−10.9, 68.2)	0.15
	FA	R	−5.5 (−54.7, 43.7)	0.83	−7.1 (−55.7, 41.5)	0.77	−9.6 (−59.9, 40.8)	0.71	−3.0 (−50.5, 44.5)	0.90
	AD	L	14.2 (−15.1, 43.5)	0.34	8.1 (−20.9, 37.2)	0.58	9.1 (−16.9, 35.2)	0.49	13.5 (−15.7, 42.7)	0.36
	AD	R	3.7 (−27.6, 34.9)	0.82	−0.2 (−30.7, 30.3)	0.99	−2.9 (−34.1, 28.2)	0.85	4.2 (−26.8, 35.2)	0.79
	RD	L	−10.5 (−39.8, 18.8)	0.48	−11.7 (−41.6, 18.1)	0.44	−9.2 (−38.0, 19.7)	0.53	−10.8 (−40.0, 18.4)	0.47
	RD	R	3.5 (−28.0, 35.0)	0.83	1.39 (−29.9, 32.7)	0.93	1.3 (−29.5, 32.1)	0.93	2.2 (−28.5, 32.9)	0.89
	MD	L	−2.7 (−33.3, 28.0)	0.86	−6.2 (−37.7, 25.3)	0.70	−3.8 (−33.4, 25.8)	0.80	−3.2 (−33.6, 27.3)	0.84
	MD	R	4.5 (−30.0, 38.9)	0.80	1.2 (−32.8, 35.2)	0.95	0.0 (−33.1, 33.1)	0.99	3.7 (−30.1, 37.6)	0.83
	Axon Density	L	−5.9 (−39.2, 27.4)	0.73	−6.8 (−40.0, 26.5)	0.69	−7.8 (−40.2, 24.7)	0.64	−5.9 (−39.2, 27.3)	0.73
	Axon Density	R	−11.2 (−39.0, 16.5)	0.43	−13.0 (−40.5, 14.5)	0.36	−14.0 (−39.8, 11.8)	0.29	−10.4 (−38.1, 17.2)	0.46
	Axon Dispersion	L	−41.5 (−91.1, 8.2)	0.10	−31.7 (−79.4, 16.0)	0.19	−21.5 (−73.1, 30.0)	0.41	−41.6 (−90.4, 7.2)	0.10
	Axon Dispersion	R	−30.5 (−95.7, 34.7)	0.36	−23.9 (−84.8, 36.9)	0.44	−9.8 (−78.5, 58.9)	0.78	−33.0 (−96.5, 30.4)	0.31

Note. Estimates of regression coefficients from separate linear regression models for each predictor-outcome combination for the left and right hemisphere. CI = confidence interval, FA = Fractional anisotropy, AD = axial diffusivity, RD = radial diffusivity, MD = mean diffusivity, L = left hemisphere, R = right hemisphere, VPT = very preterm. [a] Analyses adjusted for age, sex, language spoken at home, parental education. [b] Analyses adjusted for age, sex, language spoken at home, parental education and head motion. [c] Analyses excluding children with low IQ, imputed language score, and major brain injuries.

with language processing in widespread regions. Owing to the accumulating body of evidence from neuroscientific studies, the strictly localist view of the neural representation of language has long given way to distributed network perspectives (Dick and Tremblay, 2012; Friederici et al., 2017). Our results are in line with previous DTI studies, which found relationships between RD and phonological awareness in the corpus callosum in school-aged term-born children (Dougherty et al., 2007) and between FA and verbal IQ, linguistic processing speed as well as syntactic decoding in widespread areas of the corpus callosum, forceps, anterior thalamic radiation and corticospinal tract in 9–16 year old preterm children (Feldman et al., 2012). It is probable that the widespread tracts associated with language in younger samples reflect the ongoing specification of neural tracts (Brauer et al., 2011). Further, our language measures are multidimensional and not only contingent on specific language abilities but also dependent on other cognitive processes, such as working memory, attention, and sequencing. Interestingly, white matter microstructure in both hemispheres was associated with the language domains measured in our study. Neither whole-brain nor tract-based analyses showed clear laterality of the regions associated with semantics, grammar and phonological processing. Right-hemispheric involvement in language processing has previously been suggested in healthy term-born 4–6 year old children (O'Muircheartaigh et al., 2013; Raschle et al., 2011; Vandermosten et al., 2015) and evidence from functional imaging studies suggests increasing lateralisation of language with age, even during late childhood and adolescence (Everts et al., 2009; Mürner-Lavanchy et al., 2014b; Ressel et al., 2008; Szaflarski et al., 2006). Language development and lateralisation thus extends well beyond the time of obvious language acquisition during early childhood (Lidzba et al., 2011). Our results might therefore reflect a typical transition from a bilateral language organisation to a specialised more left-lateralised network or indicate the dependence of our language measures on other involved cognitive processes.

Secondary analyses controlling for sex, language spoken at home, parental education or head motion during scanning, revealed very similar findings to the original analyses, which were only controlled for age. Hence, widespread associations between white matter microstructure and language occured in VPT and term-born children independently from these potential confounding variables. Additional secondary analyses excluding children with major brain pathology and functionally impaired children revealed similar findings for the arcuate fasciculus tractography analysis. Excluding these children from the TBSS analysis, however, revealed less widespread associations restricted to FA for better semantic performance, lower RD for better grammar performance, and higher FA and lower RD for better phonological awareness, in regions including the corpus callosum, inferior fronto-occipital fasciculus, superior longitudinal fasciculus and uncinate fasciculus. Possible explanations for this are that the widespread associations found in our original analyses were influenced by these children with brain abnormalities and/or functional impairments, and/or by partial volume effects associated with neonatal brain abnormalities, for example, larger ventricles.

4.1. Limitations

There are some limitations with our diffusion image pre-processing and analysis. We did not acquire diffusion images with reversed phase-encode blips, so we were not able to correct for susceptibility-induced geometric distortions, as described in Andersson et al. (2003). Methodological limitations of TBSS limit the interpretation of our findings (Bach et al., 2014). The skeletonisation step introduces a spatial heterogeneity so that associations will inherently be stronger in tracts with more variability in anatomical location, which might limit the reliability of the results (Edden and Jones, 2011). Further, confining the spatial location of the analysis to a skeleton may result in a lack of specificity (Jones and Cercignani, 2010). A further limitation is the inherent challenge of inferring underlying biological substrates from changes in the diffusion parameters studied in the current paper, and care must be taken when interpreting the current findings, because it is not possible to attribute any single diffusion parameter to a specific cellular property (Bach et al., 2014; Jones et al., 2013). Despite these limitations, TBSS remains an unparalleled in vivo method for exploratory investigations of white matter, but replication of findings is strongly encouraged (Jones et al., 2013). We aimed to alleviate some of these limitations by using a more specific tract-based analysis for structure-function associations by probabilistic tracking of the arcuate fasciculus.

NODDI also has its limitations. It has been criticised for modelling the neurite orientation distribution with a single Watson distribution and consequently does not account for fibre crossings, which are a distinctive feature of human connectional neuroanatomy (Kaden et al., 2016). Further, NODDI assumes a single and fixed intrinsic diffusivity for nervous tissue over the whole brain, across MRI protocols, individuals of different age and patients with different neurological conditions, which has been argued to be a major source of the systematic overestimation of free-water content in the cerebral white matter (Kaden et al., 2016). Lastly, the NODDI method assumes that the extra-neurite water pool is in fast exchange across all neurite orientations, which has been doubted. However, our use of NODDI provided increased specificity for microstructural changes compared with DTI alone (Zhang et al., 2012).

Our main analyses combined both the VPT and term-born groups as we found little evidence that the association between white matter microstructure and language varied by birth group. We acknowledge, however, that our results might be largely driven by associations within the VPT group given the larger sample size in this group and that we may have been underpowered to detect interactions of birth group with the associations between white matter microstructure and language outcomes.

While 88% of VPT children were assessed for the 7-year follow-up, only 64% of the originally recruited VPT children had complete, usable diffusion data and were included in the current study. Differences between participating and non-participating children might lead to an overestimation of language outcomes in VPT participants in this study. Despite this, major birth characteristics such as GA at birth, birth weight or neonatal complications (IVH grade III/IV) were comparable between the participating and non-participating children, suggesting that the study sample was reasonably representative of the main study population.

In the current study, we have analysed the separate effects of multiple white matter microstructural measures on multiple language subdomains in VPT children. Future studies using more advanced statistical analysis techniques, such as those implemented in FSL's PALM tool, would be valuable to correct for multiple comparisons across the various white matter microstructural measures and language sub-scales, to examine the interrelationships between the white matter microstructural measures, and to determine whether the white matter microstructural measures have combined effects on language outcomes in VPT children (Winkler et al., 2018, 2016).

Tractography studies in healthy adults have shown that arcuate fasciculus subdivisions can be differentially related to language functions (Saur et al., 2008). Hence, subdivision analysis, using techniques such as that by Yeatman et al. (2011) might yield more detailed insight into how arcuate fasciculus microstructure is related to language in children. The functional segregation of subdivisions can, however, result from artificial experimental situations. Arguably, in naturally occurring speech, complex interactions and the involvement of different subdivisions of tracts lead to proficiency in verbal communication (Saur et al., 2008).

Studies investigating associations between FA and language in VPT adolescents have found tracts other than the arcuate fasciculus to be associated with language abilities, namely the left uncinate fasciculus

and forceps minor with receptive vocabulary, the right inferior fronto-occipital fasciculus with syntactic comprehension and the body and genu of the corpus callosum with word identification (Feldman et al., 2012; Mullen et al., 2011) (see Pandit et al., 2013 for a review). Recent evidence from studies in healthy term-born children further suggests there is an additional ventral language pathway connecting the anterior temporal lobe with the inferior frontal gyrus over the uncinate fasciculus (Vandermosten et al., 2015). Further investigation of white matter tracts potentially involved in language in VPT children apart from the arcuate fasciculus using tractography would be worth while in future.

4.2. Conclusions

Whole-brain TBSS analyses of DTI and NODDI parameters illustrate widespread associations between white matter microstructure and language outcomes, suggesting that white matter organisation is related to language in VPT and term-born children. Tractography analyses further suggest that white matter microstructural organisation in the arcuate fasciculus is related to better language outcome.

Conflict of interest

Conflicts of interest: none.

Acknowledgements

We are indebted to the physicians, psychometricians, psychologists, research coordinators and all other staff who made this study possible; and most importantly, to the children and their families who participated in this follow-up study. The funding sources had no involvement in the study design; in the collection, analysis and interpretation of data; in the writing of the report; and in the decision to submit the article for publication.

Funding

Contract grant sponsor: National Institutes of Health (NIH); Contract grant numbers: R01 HD05709801, P30 HD062171, and UL1 TR000448 to T.E.I.;

Contract grant sponsor: The National Health and Medical Research Council (NHMRC) of Australia; Contract grant number: Project Grant No. 237117 to T.E.I. and L.W.D.; Project Grant No. 491209 to P.J.A., T.E.I. and L.W.D.; Project Grant No. 607315 and 1105008 to A.T.M.

Contract grant sponsor: The NHMRC of Australia Centre of Research Excellence; Contract grant number: No. 1060733 to L.W.D., P.J.A, J.L.Y·C. and D.K.T.;

Contract grant sponsor: The NHMRC of Australia Senior Research Fellowship; Contract grant number: No. 1081288 to P.J.A.

Contract grant sponsor: The NHMRC of Australia Career Development Fellowship; Contract grant number: No. 1085754 to D.K.T.; Contract grant number: No. 1053609 to K.J.L.

Contract grant sponsor: The NHMRC of Australia Early Career Fellowship; Contract grant numbers: No. 1012236 to D.K.T. and 1053787 to J.L.Y.C;

Contract grant sponsor: the United Cerebral Palsy Foundation, The United States to T.E.I.

Appendix A. Supplementary data

Supplementary data to this article can be found online at https://doi.org/10.1016/j.nicl.2018.09.020.

References

Andersson, J.L.R., Skare, S., Ashburner, J., 2003. How to correct susceptibility distortions in spin-echo echo-planar images: application to diffusion tensor imaging. NeuroImage 20, 870–888. https://doi.org/10.1016/S1053-8119(03)00336-7.

Andersson, J.L.R., Jenkinson, M., Smith, S., Andersson, J., 2007a. Non-linear Registration Aka Spatial Normalisation FMRIB Technial Report TR07JA2. FMRIB Centre, Oxford, United Kingdom.

Andersson, J.L.R., Jenkinson, M., Smith, S., Andersson, J., 2007b. Non-linear Optimisation FMRIB Technial Report TR07JA1. In: FMRIB Centre. United Kingdom, Oxford.

Avants, B.B., Epstein, C.L., Grossman, M., Gee, J.C., 2008. Symmetric diffeomorphic image registration with cross-correlation: evaluating automated labeling of elderly and neurodegenerative brain. Med. Image Anal. 12, 26–41. https://doi.org/10.1016/j.media.2007.06.004.

Bach, M., Laun, F.B., Leemans, A., Tax, C.M.W., Biessels, G.J., Stieltjes, B., Maier-Hein, K.H., 2014. Methodological considerations on tract-based spatial statistics (TBSS). NeuroImage 100, 358–369. https://doi.org/10.1016/j.neuroimage.2014.06.021.

Barre, N., Morgan, A., Doyle, L.W., Anderson, P.J., 2011. Language abilities in children who were very preterm and/or very low birth weight: a meta-analysis. J. Pediatr. 158, 766–774.e1. https://doi.org/10.1016/j.jpeds.2010.10.032.

Bernal, B., Altman, N., 2010. The connectivity of the superior longitudinal fasciculus: a tractography DTI study. Magn. Reson. Imaging 28, 217–225. https://doi.org/10.1016/j.mri.2009.07.008.

Brauer, J., Anwander, A., Friederici, A.D., 2011. Neuroanatomical prerequisites for language functions in the maturing brain. Cereb. Cortex 21, 459–466. https://doi.org/10.1093/cercor/bhq108.

Carlin, J.B., Gurrin, L.C., Sterne, J.A., Morley, R., Dwyer, T., 2005. Regression models for twin studies: a critical review. Int. J. Epidemiol. 34, 1089–1099. https://doi.org/10.1093/ije/dyi153.

Carroll, J.M., Maughan, B., Goodman, R., Meltzer, H., 2005. Literacy difficulties and psychiatric disorders: evidence for comorbidity. J. Child Psychol. Psychiatry 46, 524–532. https://doi.org/10.1111/j.1469-7610.2004.00366.x.

Catani, M., Jones, D.K., Ffytche, D.H., 2005. Perisylvian language networks of the human brain. Ann. Neurol. 57, 8–16. https://doi.org/10.1002/ana.20319.

Cheong, J.L.Y., Thompson, D.K., Wang, H.X., Hunt, R.W., Anderson, P.J., Inder, T.E., Doyle, L.W., 2009. Abnormal white matter signal on MR imaging is related to abnormal tissue microstructure. Am. J. Neuroradiol. 30, 623–628. https://doi.org/10.3174/ajnr.A1399.

Constable, R.T., Vohr, B.R., Scheinost, D., Benjamin, J.R., Fulbright, R.K., Lacadie, C., Schneider, K.C., Katz, K.H., Zhang, H., Papademetris, X., Ment, L.R., 2013. A left cerebellar pathway mediates language in prematurely-born young adults. NeuroImage 64, 371–378. https://doi.org/10.1016/j.neuroimage.2012.09.008.

Deoni, S.C.L., Rutt, B.K., Arun, T., Pierpaoli, C., Jones, D.K., 2008. Gleaning multicomponent T1 and T2 information from steady-state imaging data. Magn. Reson. Med. 60, 1372–1387. https://doi.org/10.1002/mrm.21704.

Dick, A.S., Tremblay, P., 2012. Beyond the arcuate fasciculus: consensus and controversy in the connectional anatomy of language. Brain 135, 3529–3550. https://doi.org/10.1093/brain/aws222.

Dodson, C.K., Travis, K.E., Borchers, L.R., Marchman, V.A., Ben-Shachar, M., Feldman, H.M., 2018. White matter properties associated with pre-reading skills in 6-year-old children born preterm and at term. Dev. Med. Child Neurol. 1–8. https://doi.org/10.1111/dmcn.13783.

Dougherty, R.F., Ben-Shachar, M., Deutsch, G.K., Hernandez, A., Fox, G.R., Wandell, B.A., 2007. Temporal-callosal pathway diffusivity predicts phonological skills in children. Proc. Natl. Acad. Sci. 104, 8556–8561. https://doi.org/10.1073/pnas.0608961104.

Edden, R.A., Jones, D.K., 2011. Spatial and orientational heterogeneity in the statistical sensitivity of skeleton-based analyses of diffusion tensor MR imaging data. J. Neurosci. Methods 201, 213–219. https://doi.org/10.1016/j.jneumeth.2011.07.025.

Everts, R., Lidzba, K., Wilke, M., Kiefer, C., Mordasini, M., Schroth, G., Perrig, W., Steinlin, M., 2009. Strengthening of laterality of verbal and visuospatial functions during childhood and adolescence. Hum. Brain Mapp. 30, 473–483. https://doi.org/10.1002/hbm.20523.

Feldman, H.M., Lee, E.S., Yeatman, J.D., Yeom, K.W., 2012. Language and reading skills in school-aged children and adolescents born preterm are associated with white matter properties on diffusion tensor imaging. Neuropsychologia 50, 3348–3362. https://doi.org/10.1016/j.neuropsychologia.2012.10.014.

Foster-Cohen, S.H., Friesen, M.D., Champion, P.R., Woodward, L.J., 2010. High prevalence/low severity language delay in preschool children born very preterm. J. Dev. Behav. Pediatr. 31, 658–667. https://doi.org/10.1097/DBP.0b013e3181e5ab7e.

Friederici, A.D., 2011. The brain basis of language processing: from structure to function. Physiol. Rev. 91, 1357–1392. https://doi.org/10.1152/physrev.00006.2011.

Friederici, A.D., Chomsky, N., Berwick, R.C., Moro, A., Bolhuis, J.J., 2017. Language, mind and brain. Nat. Hum. Behav. 1. https://doi.org/10.1038/s41562-017-0184-4.

Frye, R.E., Hasan, K., Malmberg, B., Desouza, L., Swank, P., Smith, K., Landry, S., 2010. Superior longitudinal fasciculus and cognitive dysfunction in adolescents born preterm and at term. Dev. Med. Child Neurol. 52, 760–766. https://doi.org/10.1111/j.1469-8749.2010.03633.x.

Ganzetti, M., Wenderoth, N., Mantini, D., 2014. Whole brain myelin mapping using T1- and T2-weighted MR imaging data. Front. Hum. Neurosci. 8, 671. https://doi.org/10.3389/fnhum.2014.00671.

Glasser, M.F., Van Essen, D.C., 2011. Mapping human cortical areas in vivo based on myelin content as revealed by T1- and T2-weighted MRI. J. Neurosci. 31, 11597–11616. https://doi.org/10.1523/JNEUROSCI.2180-11.2011.

Guarini, A., Sansavini, A., Fabbri, C., Alessandroni, R., Faldella, G., Karmiloff-Smith, A., 2009. Reconsidering the impact of preterm birth on language outcome. Early Hum. Dev. 85, 639–645. https://doi.org/10.1016/j.earlhumdev.2009.08.061.

Hong, J.H., Kim, S.H., Ahn, S.H., Jang, S.H., 2009. The anatomical location of the arcuate fasciculus in the human brain: a diffusion tensor tractography study. Brain Res. Bull.

80, 52–55. https://doi.org/10.1016/j.brainresbull.2009.05.011.
Hua, K., Zhang, J., Wakana, S., Jiang, H., Li, X., Reich, D.S., Calabresi, P.A., Pekar, J.J., van Zijl, P.C.M., Mori, S., 2008. Tract probability maps in stereotaxic spaces: analyses of white matter anatomy and tract-specific quantification. NeuroImage 39, 336–347. https://doi.org/10.1016/j.neuroimage.2007.07.053.
Inder, T.E., Wells, S.J., Mogridge, N.B., Spencer, C., Volpe, J.J., 2003. Defining the nature of the cerebral abnormalities in the premature infant: a qualitative magnetic resonance imaging study. J. Pediatr. 143, 171–179. https://doi.org/10.1067/S0022-3476(03)00357-3.
Jenkinson, M., Bannister, P., Brady, M., Smith, S., 2002. Improved optimization for the robust and accurate linear registration and motion correction of brain images. NeuroImage 17, 825–841.
Jones, D.K., Cercignani, M., 2010. Twenty-five pitfalls in the analysis of diffusion MRI data. NMR Biomed. 23, 803–820. https://doi.org/10.1002/nbm.1543.
Jones, D.K., Knösche, T.R., Turner, R., 2013. White matter integrity, fiber count, and other fallacies: the do's and don'ts of diffusion MRI. NeuroImage 73, 239–254. https://doi.org/10.1016/j.neuroimage.2012.06.081.
Kaden, E., Kelm, N.D., Carson, R.P., Does, M.D., Alexander, D.C., 2016. NeuroImage Multi-compartment microscopic diffusion imaging. NeuroImage 139, 346–359. https://doi.org/10.1016/j.neuroimage.2016.06.002.
Kelly, C.E., Thompson, D.K., Chen, J., Leemans, A., Adamson, C.L., Inder, T.E., Cheong, J.L.Y., Doyle, L.W., Anderson, P.J., 2016. Axon density and axon orientation dispersion in children born preterm. Hum. Brain Mapp. 37, 3080–3102. https://doi.org/10.1002/hbm.23227.
Korkman, M., Kirk, U., Kemp, S., 2007. NEPSY-II. In: Harcourt Assessment, San Antonio, TX, 2nd ed. .
Lebel, C., Beaulieu, C., 2009. Lateralization of the arcuate fasciculus from childhood to adulthood and its relation to cognitive abilities in children. Hum. Brain Mapp. 30, 3563–3573. https://doi.org/10.1002/hbm.20779.
Lebel, C., Deoni, S., 2018. The development of brain white matter microstructure. NeuroImage. https://doi.org/10.1016/j.neuroimage.2017.12.097.
Leemans, A., Jones, D.K., 2009. The B-matrix must be rotated when correcting for subject motion in DTI data. Magn. Reson. Med. 61, 1336–1349. https://doi.org/10.1002/mrm.21890.
Lidzba, K., Schwilling, E., Grodd, W., Krägeloh-Mann, I., Wilke, M., 2011. Language comprehension vs. language production: Age effects on fMRI activation. Brain Lang. 119, 6–15. https://doi.org/10.1016/j.bandl.2011.02.003.
Lubsen, J., Vohr, B., Myers, E., Hampson, M., Lacadie, C., Schneider, K.C., Katz, K.H., Constable, R.T., Ment, L.R., 2011. Microstructural and functional connectivity in the developing preterm brain. Semin. Perinatol. 35, 34–43. https://doi.org/10.1053/j.semperi.2010.10.006.
Matsumoto, R., Okada, T., Mikuni, N., Mitsueda-Ono, T., Taki, J., Sawamoto, N., Hanakawa, T., Miki, Y., Hashimoto, N., Fukuyama, H., Takahashi, R., Ikeda, A., 2008. Hemispheric asymmetry of the arcuate fasciculus. J. Neurol. 255, 1703–1711. https://doi.org/10.1007/s00415-008-0005-9.
Ment, L.R., Hirtz, D., Hüppi, P.S., 2009. Imaging biomarkers of outcome in the developing preterm brain. Lancet Neurol. 8, 1042–1055. https://doi.org/10.1016/S1474-4422(09)70257-1.
Miller, S.P., Ferriero, D.M., Leonard, C., Piecuch, R., Glidden, D.V., Partridge, J.C., Perez, M., Mukherjee, P., Vigneron, D.B., Barkovich, A.J., 2005. Early brain injury in premature newborns detected with magnetic resonance imaging is associated with adverse early neurodevelopmental outcome. J. Pediatr. 147, 609–616. https://doi.org/10.1016/j.jpeds.2005.06.033.
Mullen, K.M., Vohr, B.R., Katz, K.H., Schneider, K.C., Lacadie, C., Hampson, M., Makuch, R.W., Reiss, A.L., Constable, R.T., Ment, L.R., 2011. Preterm birth results in alterations in neural connectivity at age 16 years. NeuroImage 54, 2563–2570. https://doi.org/10.1016/j.neuroimage.2010.11.019.
Mürner-Lavanchy, I., Steinlin, M., Kiefer, C., Weisstanner, C., Ritter, B.C., Perrig, W., Everts, R., 2014a. Delayed Development of Neural Language Organization in Very Preterm Born Children. Dev. Neuropsychol. 39, 529–542. https://doi.org/10.1080/87565641.2014.959173.
Mürner-Lavanchy, I., Steinlin, M., Nelle, M., Rummel, C., Perrig, W.J., Schroth, G., Everts, R., 2014b. Delay of cortical thinning in very preterm born children. Early Hum. Dev. 90, 443–450. https://doi.org/10.1016/j.earlhumdev.2014.05.013.
Murray, A.L., Thompson, D.K., Pascoe, L., Leemans, A., Inder, T.E., Doyle, L.W., Anderson, J.F.I., Anderson, P.J., 2016. White matter abnormalities and impaired attention abilities in children born very preterm. NeuroImage 124, 75–84. https://doi.org/10.1016/j.neuroimage.2015.08.044.
Nagy, Z., Westerberg, H., Skare, S., Andersson, J.L., Lilja, A., et al., 2003. Preterm children have disturbances of white matter at 11 years of age as shown by diffusion tensor imaging. Pediatric Research 54, 672–679.
Nichols, T.E., Holmes, A.P., 2002. Nonparametric permutation tests for functional neuroimaging: a primer with examples. Hum. Brain Mapp. 15, 1–25.
van Noort-van der Spek, I.L., Franken, M.-C.J.P., Weisglas-Kuperus, N., 2012. Language functions in preterm-born children: a systematic review and meta-analysis. Pediatrics 129, 745–754. https://doi.org/10.1542/peds.2011-1728.
Northam, G.B., Liégeois, F., Chong, W.K., Baker, K., Tournier, J.D., Wyatt, J.S., Baldeweg, T., Morgan, A., 2012a. Speech and oromotor outcome in adolescents born preterm: Relationship to motor tract integrity. J. Pediatr. 160, 402–409. https://doi.org/10.1016/j.jpeds.2011.08.055.
Northam, G.B., Liégeois, F., Tournier, J.-D., Croft, L.J., Johns, P.N., Chong, W.K., Wyatt, J.S., Baldeweg, T., 2012b. Interhemispheric temporal lobe connectivity predicts language impairment in adolescents born preterm. Brain 135, 3781–3798. https://doi.org/10.1093/brain/aws276.
O'Muircheartaigh, J., Dean, D.C., Dirks, H., Waskiewicz, N., Lehman, K., Jerskey, B.A., Deoni, S.C.L., Deoni, S.C.L., 2013. Interactions between white matter asymmetry and language during neurodevelopment. J. Neurosci. 33, 16170–16177. https://doi.org/10.1523/JNEUROSCI.1463-13.2013.
Pandit, A.S., Ball, G., Edwards, A.D., Counsell, S.J., 2013. Diffusion magnetic resonance imaging in preterm brain injury. Neuroradiology 55. https://doi.org/10.1007/s00234-013-1242-x.
Perani, D., Saccuman, M.C., Scifo, P., Anwander, A., Spada, D., Baldoli, C., Poloniato, A., Lohmann, G., Friederici, A.D., 2011. Neural language networks at birth. Proc. Natl. Acad. Sci. 108, 16056–16061. https://doi.org/10.1073/pnas.1102991108.
Raschle, N.M., Chang, M., Gaab, N., 2011. Structural brain alterations associated with dyslexia predate reading onset. NeuroImage 57, 742–749. https://doi.org/10.1016/j.neuroimage.2010.09.055.
Reidy, N., Morgan, A., Thompson, D.K., Inder, T.E., Doyle, L.W., Anderson, P.J., 2013. Impaired language abilities and white matter abnormalities in children born very preterm and/or very low birth weight. J. Pediatr. 162, 719–724. https://doi.org/10.1016/j.jpeds.2012.10.017.
Ressel, V., Wilke, M., Lidzba, K., Lutzenberger, W., Krägeloh-Mann, I., 2008. Increases in language lateralization in normal children as observed using magnetoencephalography. Brain Lang. 106, 167–176. https://doi.org/10.1016/j.bandl.2008.01.004.
Salvan, P., Tournier, J.D., Batalle, D., Falconer, S., Chew, A., Kennea, N., Aljabar, P., Dehaene-Lambertz, G., Arichi, T., Edwards, A.D., Counsell, S.J., 2017. Language ability in preterm children is associated with arcuate fasciculi microstructure at term. Hum. Brain Mapp. 38, 3836–3847. https://doi.org/10.1002/hbm.23632.
Saur, D., Kreher, B.W., Schnell, S., Kummerer, D., Kellmeyer, P., Vry, M.-S., Umarova, R., Musso, M., Glauche, V., Abel, S., Huber, W., Rijntjes, M., Hennig, J., Weiller, C., 2008. Ventral and dorsal pathways for language. Proc. Natl. Acad. Sci. 105, 18035–18040. https://doi.org/10.1073/pnas.0805234105.
Saygin, Z.M., Norton, E.S., Osher, D.E., Beach, S.D., Cyr, A.B., Ozernov-Palchik, O., Yendiki, A., Fischl, B., Gaab, N., Gabrieli, J.D.E., 2013. Tracking the roots of reading ability: white matter volume and integrity correlate with phonological awareness in prereading and early-reading kindergarten children. J. Neurosci. 33, 13251–13258. https://doi.org/10.1523/JNEUROSCI.4383-12.2013.
Semel, E., Wiig, E.H., Secord, W., 2006. Clinical Evaluation of Language Fundamentals, 4th ed. Harcourt Assessment, Marrackville, Australia.
Skeide, M.A., Brauer, J., Friederici, A.D., 2016. Brain functional and structural predictors of language performance. Cereb. Cortex 26, 2127–2139. https://doi.org/10.1093/cercor/bhv042.
Skranes, J., Vangberg, T.R., Kulseng, S., Indredavik, M.S., Evensen, K.A.I., Martinussen, M., Dale, A.M., Haraldseth, O., Brubakk, A.-M., 2007. Clinical findings and white matter abnormalities seen on diffusion tensor imaging in adolescents with very low birth weight. Brain 130, 654–666. https://doi.org/10.1093/brain/awm001.
Smith, S., Nichols, T., 2009. Threshold-free cluster enhancement: addressing problems of smoothing, threshold dependence and localisation in cluster inference. NeuroImage 44, 83–98. https://doi.org/10.1016/j.neuroimage.2008.03.061.
Smith, S.M., Jenkinson, M., Johansen-Berg, H., Rueckert, D., Nichols, T.E., MacKay, C.E., Watkins, K.E., Ciccarelli, O., Cader, M.Z., Matthews, P.M., Behrens, T.E.J., 2006. Tract-based spatial statistics: Voxelwise analysis of multi-subject diffusion data. NeuroImage 31, 1487–1505. https://doi.org/10.1016/j.neuroimage.2006.02.024.
Song, S.-K., Sun, S.-W., Ju, W.-K., Lin, S.-J., Cross, A.H., Neufeld, A.H., 2003. Diffusion tensor imaging detects and differentiates axon and myelin degeneration in mouse optic nerve after retinal ischemia. NeuroImage 20, 1714–1722.
StataCorp, 2013. Stata Statistical Software: Release 13. StataCorp LP, College Station, TX.
Szaflarski, J.P., Holland, S.K., Schmithorst, V.J., Byars, A.W., 2006. fMRI study of language lateralization in children and adults. Hum. Brain Mapp. 27, 202–212. https://doi.org/10.1002/hbm.20177.
Thompson, D.K., Lee, K.J., Egan, G.F., Warfield, S.K., Doyle, L.W., Anderson, P.J., Inder, T.E., 2014. Regional white matter microstructure in very preterm infants: Predictors and 7 year outcomes. Cortex 52, 60–74. https://doi.org/10.1016/j.cortex.2013.11.010.
Tournier, J.D., 2010. MRtrix Package. Brain Research Institute, Melbourne, Australia.
Tournier, J.-D., Calamante, F., Gadian, D.G., Connelly, A., 2004. Direct estimation of the fiber orientation density function from diffusion-weighted MRI data using spherical deconvolution. NeuroImage 23, 1176–1185. https://doi.org/10.1016/j.neuroimage.2004.07.037.
Tournier, J.-D., Calamante, F., Connelly, A., 2007. Robust determination of the fibre orientation distribution in diffusion MRI: Non-negativity constrained super-resolved spherical deconvolution. NeuroImage 35, 1459–1472. https://doi.org/10.1016/j.neuroimage.2007.02.016.
Tournier, J.-D., Calamante, F., Connelly, A., 2012. MRtrix: diffusion tractography in crossing fiber regions. Int. J. Imaging Syst. Technol. 22, 53–66. https://doi.org/10.1002/ima.22005.
Travis, K.E., Ben-Shachar, M., Myall, N.J., Feldman, H.M., 2016. Variations in the neurobiology of reading in children and adolescents born full term and preterm. NeuroImage Clin. 11, 555–565. https://doi.org/10.1016/j.nicl.2016.04.003.
Turken, A.U., Dronkers, N.F., 2011. The neural architecture of the language comprehension network: converging evidence from lesion and connectivity analyses. Front. Syst. Neurosci. 5, 1. https://doi.org/10.3389/fnsys.2011.00001.
Vandermosten, M., Boets, B., Poelmans, H., Sunaert, S., Wouters, J., Ghesquiere, P., 2012. A tractography study in dyslexia: neuroanatomic correlates of orthographic, phonological and speech processing. Brain 135, 935–948. https://doi.org/10.1093/brain/awr363.
Vandermosten, M., Vanderauwera, J., Theys, C., De Vos, A., Vanvooren, S., Sunaert, S., Wouters, J., Ghesquière, P., 2015. A DTI tractography study in pre-readers at risk for dyslexia. Dev. Cogn. Neurosci. 14, 8–15. https://doi.org/10.1016/j.dcn.2015.05.006.
Veraart, J., Sijbers, J., Sunaert, S., Leemans, A., Jeurissen, B., 2013. Weighted linear least squares estimation of diffusion MRI parameters: strengths, limitations, and pitfalls. NeuroImage 81. https://doi.org/10.1016/j.neuroimage.2013.05.028.

Volpe, J., 2009a. Brain injury in premature infants: a complex amalgam of destructive and developmental disturbances. Lancet Neurol. 8, 110–124. https://doi.org/10.1016/S1474-4422(08)70294-1.

Volpe, J., 2009b. The encephalopathy of prematurity-brain injury and impaired brain development inextricably intertwined. Semin. Pediatr. Neurol. 16, 167–178. https://doi.org/10.1016/j.spen.2009.09.005.

Walton, M., Dewey, D., Lebel, C., 2018. Brain white matter structure and language ability in preschool-aged children. Brain Lang. 176, 19–25. https://doi.org/10.1016/j.bandl.2017.10.008.

Wasserstein, R.L., Lazar, N.A., 2016. The ASA's Statement on p-Values: Context, Process, and Purpose. Am. Stat. 70, 129–133. https://doi.org/10.1080/00031305.2016.1154108.

Wiig, E.H., Secord, W., 1989. Test of language competence - expanded edition. The Psychological Corporation, San Antonio, TX.

Winkler, A.M., Ridgway, G.R., Webster, M.A., Smith, S.M., Nichols, T.E., 2014. Permutation inference for the general linear model. NeuroImage 92, 381–397. https://doi.org/10.1016/j.neuroimage.2014.01.060.

Winkler, A.M., Greve, D.N., Bjuland, K.J., Nichols, T.E., Sabuncu, M.R., Håberg, A.K., Skranes, J., Rimol, L.M., 2018. Joint Analysis of Cortical Area and Thickness as a Replacement for the Analysis of the volume of the Cerebral Cortex. Cereb. Cortex 28, 738–749. https://doi.org/10.1093/cercor/bhx308.

Wolke, D., Samara, M., Bracewell, M., Marlow, N., 2008. Specific Language difficulties and school achievement in children born at 25 weeks of gestation or less. J. Pediatr. 152. https://doi.org/10.1016/j.jpeds.2007.06.043.

Yeatman, J.D., Dougherty, R.F., Rykhlevskaia, E., Sherbondy, A.J., Deutsch, G.K., Wandell, B.A., Ben-Shachar, M., 2011. Anatomical properties of the arcuate fasciculus predict phonological and reading skills in children. J. Cogn. Neurosci. 23, 3304–3317. https://doi.org/10.1162/jocn_a_00061.

Yendiki, A., Koldewyn, K., Kakunoori, S., Kanwisher, N., Fischl, B., 2014. Spurious group differences due to head motion in a diffusion MRI study. NeuroImage 88, 79–90. https://doi.org/10.1016/j.neuroimage.2013.11.027.

Zhang, H., Schneider, T., Wheeler-Kingshott, C.A., Alexander, D.C., 2012. NODDI: Practical in vivo neurite orientation dispersion and density imaging of the human brain. NeuroImage 61, 1000–1016. https://doi.org/10.1016/j.neuroimage.2012.03.072.